JACS
JOURNAL OF THE AMERICAN CHEMICAL SOCIETY

ARTICLE

pubs.acs.org/JACS

Electrical Detection of Single Methylcytosines in a DNA Oligomer

Makusu Tsutsui,[†] Kazuki Matsubara,[†] Takahito Ohshiro,[†] Masayuki Furuhashi,[†] Masateru Taniguchi,[*,†] and Tomoji Kawai[*,†,‡]

[†]The Institute of Scientific and Industrial Research, Osaka University, 8-1 Mihogaoka, Ibaraki, Osaka 567-0047, Japan

[‡]Division of Quantum Phases and Devices, Department of Physics, Konkuk University, Seoul 143-701, Republic of Korea

Supporting Information

ABSTRACT: We report label-free electrical detections of chemically modified nucleobases in a DNA using a nucleotide-sized electrode gap. We found that methyl substitution contributes to increase the tunneling conductance of deoxycytidines, which was attributed to a shift of the highest occupied molecular orbital level closer to the electrode Fermi level by methylation. We also demonstrate statistical identifications of methylcytosines in an oligonucleotide by tunneling current. This result suggests a possible use of the transverse electron-transport method for a methylation level analysis.

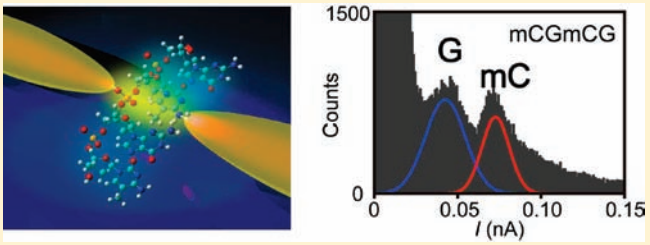

INTRODUCTION

Completion of the human genome sequence has revealed the complexities of how the hereditary information is stored in our DNA; in addition to the sequence of the four nucleosides, it is now known that chemically modified nucleobases also play a crucial role in gene expression.[1−5] Among DNA modifications, DNA methylation constitutes an essential epigenetic mechanism for various important biological processes such as embryonic development, replications, and aging and is the most extensively studied epigenetic mark because of the direct relevance to human health and disease.[4−6] Interpreting its epigenetic function is a formidable task that necessitates mapping of methylation patterns among the various cell types or patients.[6] Present technologies for detecting this covalent modification in DNA use chemical reactions to label or convert target nucleobases in prior to sequence analysis.[4,5,7] This is due to the fact that there is no sequencing technology capable of identifying the small change in chemical and electrical characteristics of base molecules in a DNA sequence associated with single substitutions in their native form. On the other hand, the single-molecule electrical approach has proven to be promising in directly interrogating a DNA sequence without labelings and PCR amplifications.[8−10] Particularly, tunneling current is a very sensitive probe for detecting a minute difference in molecular electronic structure at a single-molecule level.[11−18]

In the present work, we demonstrate a direct electrical detection of cytosine methylation in a single-molecule short DNA by tunneling current using a pair of Au electrodes (Figure 1a); as methylation is anticipated to affect the π-conjugation of the pyrimidine (or purine) bases considering the electron-donating character of methyl substitutions, it is expected that the electron tunneling method can be utilized for high-throughput methylation analyses. For this purpose, we first explored the effects of methylation on electrical conductivity of deoxycytidine-5′-monophosphate (dCMP) at the single-molecule level. We performed two-probe current measurements in a Milli-Q solution of methylated and nonmethylated dCMPs (1 μM) under a constant dc bias voltage of 0.4 V using a gap-tunable Au nanoelectrode system (see the Experimental Details and Supporting Information Figure S1). This method enables a reliable estimation of the tunneling conductnce of single nucleotides captured in a 1 nm electrode gap.[18]

EXPERIMENTAL DETAILS

A microfabricated mechanically controllable break junction (MCBJ) is employed to form nucleotide-sized electrode gaps. Fabrication procedures of MCBJs are described elsewhere.[19,20] First, we coated a phosphor bronze substrate with a thin polyimide layer for electrical insulation. A gold nanojunction was then fabricated by electron-beam lithography and subsequent lift-off processes. After that, the junction was exposed to an isotropic reactive ion etching using CF_4/O_2 gas by which to remove the underlying polyimide and obtain a free-standing Au nanobridge. The MCBJ sample was mounted in a three-point bending configuration (Supporting Information Figure S1a). The substrate was bent and the junction was broken mechanically so as to form a pair of Au nanoelectrodes. Meanwhile, the junction conductance was monitored using a Keithley 6487 picoammeter (Keithley) under a dc bias voltage of 0.1 V. A 10 kΩ resistor was connected in series during this process in order to protect the junction from overcurrent-induced electromigration failure. A special care was taken in the adjustment of electrode gap size by using the self-breaking technique (Supporting Information Figure S1b).[21,22]

We formed a 1 nm electrode gap in a dilute Milli-Q solution of a target nucleotide molecule at a concentration of 1 μM. Current across the electrodes was recorded at 10 kHz using a home-built logarithmic

Received: April 26, 2011
Published: May 11, 2011

dx.doi.org/10.1021/ja203839e | J. Am. Chem. Soc. 2011, 133, 9124–9128

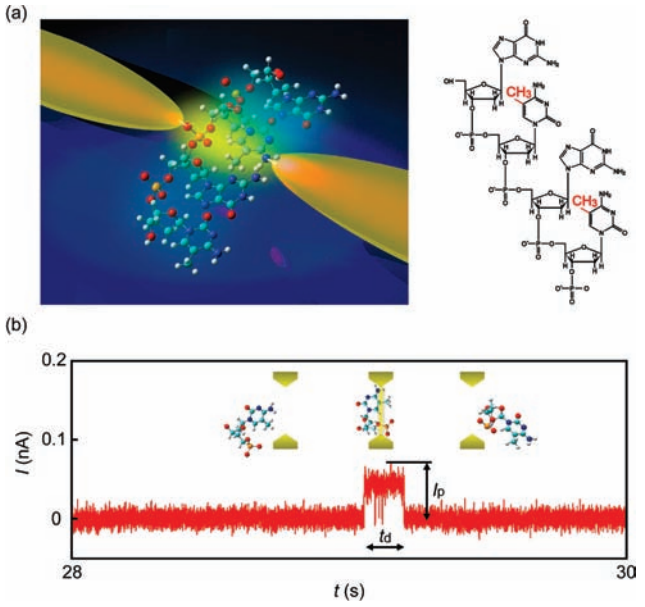

Figure 1. Single-molecule conductance of chemically modified monomer nucleotides. (a) A schematic illustration describing the two-probe current measurements of a single DNA oligomer containing methylated cytosine in the sequence using a 1 nm electrode gap. (b) A characteristic current spike obtained in a Milli-Q solution of deoxycytidines signifying trapping of a nucleotide molecule in the electrode gap. The base current is offset to zero. The schematic drawing depicts a sequential trapping and detrapping event of single methyl-dCMP in the electrode gap. Single-nucleotide detections can be achieved by monitoring the pulselike current signals characterized by the height I_p and the width t_d.

current amplifier and a PXI-4071 digital multimeter (National Instruments) under a dc bias voltage of 0.4 V. After every 1 h of $I-t$ measurement, we replaced the MCBJ sample to a new one. About 20 samples were used for each nucleotide to obtain about 1000 spikelike signals necessary for deducing the single-molecule conductance. This is to suppress a possible contamination effect on the measurements. 2′-Deoxycytidine 5′-monophosphate, 8-hydroxy-2′-deoxyguanosine, 2′-deoxyguanosine, and 2′-deoxyguanosine 5′-monophosphate were purchased from Sigma-Aldrich Co., Ltd. Methyldeoxycytidine 5′-monophosphate was provided by USB Co., Ltd. DNA 4-mer with sequences 3′-mCGmCG-5′ and 3′-GGGG-5′ were synthesized by FASMAC Co., Ltd. No buffer was added to control the protonation state of the nucleotides.

RESULTS AND DISCUSSION

Electrical Detection of Chemically Modified Single Nucleotides. Figure 1b shows a partial current trace obtained for methyl-dCMPs. We found characteristic spikelike signal in the $I-t$ curve, which signifies trapping and detrapping of single methyl-dCMPs in the electrode gap; the sharp current increase originates from a contribution of tunnelling current flowing through the single nucleotides residing in the nanospace between electrodes, whereas subsequent drops to the base current level suggest molecular escape (Figure 1b).[18] The width of each spike represents the trapping duration of single nucleotides, which typically falls in a range of 1−100 ms. We examined the molecular electron-transport characteristics by correcting the peak height I_p of each current spike signal (Figure 1b). As a reference, we also carried out the single-nucleotide detection measurements for dCMPs (Figure 2a). About a half of the 20 MCBJ-electrode gaps used for single-molecule conductance measurements of each nucleotide showed current spikes; others gave featureless $I-t$ traces suggesting formation of a larger electrode gap than the size of the nucleotides, which is around 1 nm. The rate of detecting current spikes in 1 h of $I-t$ measurement was around 1 event per 30 s on average. Short pulselike signals with a width less than 1 ms were excluded from the I_p derivation. Histograms constructed with about 1000 I_p data reveal a single peak profile (Figure 2b) with a relatively broad distribution depicting a wide variation of molecular conformation and configuration of single nucleotides in an electrode gap.[18,23−25] Here, I_p was taken in logarithmic scale. This is because it is anticipated that random Au−nucleotide−Au tunneling junction geometries were sampled in the experiments, which leads to exponential variation of I_p. The single-peak distributions suggest an existence of a stable electrode−nucleotide−electrode structure frequently formed during molecular trapping.[18,23−25] We define the conductance of this particular molecular bridge as the characteristic single-molecule tunneling conductance G. Gaussian fits to the I_p histograms provide $G_{\text{m-dCMP}}$ = 123 pS and G_{dCMP} = 78 pS for methyl-dCMP and dCMP, respectively (Figure 2b).[18] These results suggest that dCMP and methyl-dCMP can be discriminated statistically at a single-molecule level from their electrical conductivity.

The fact that $G_{\text{m-dCMP}}$ is larger than G_{dCMP} indicates a positive contribution of methylation to the electrical conductance of dCMP. The single-molecule conductance of the Au−nucleotide−Au system in the coherent tunneling regime can be described as

$$G = \frac{e^2}{\pi\hbar}\frac{\Gamma_L\Gamma_R}{(E_F - E_{HOMO})^2}$$

where E_F, $E_{HOMO(LUMO)}$, and $\Gamma_{L(R)}$ represent the Fermi energy of the electrodes, the energy of the HOMO (or LUMO), and the left (right) electrode−molecule coupling strength, respectively.[9,17,26,27] It is naturally expected that electrode−molecule coupling is essentially the same for methyl-dCMP and dCMP as these molecules share identical amine anchoring groups in common. For the energy gap $\Delta E = E_F - E_{HOMO(LUMO)}$, the highest occupied molecular orbital (HOMO) level and the lowest unoccupied molecular orbital (LUMO) level of the nucleotides were calculated at the DFT B3LYP level using the 6-31G(d,p) basis set with the Gaussian 03 program package. The results show that the HOMO of the nucleotides measured in the present work is closer to E_F than the LUMO. Therefore, the energy gap between the HOMO of nucleotides and the Au electrode Fermi level affects the electron transmissivity in the Au−nucleotide−Au structure. Assuming E_F = −5.20 eV and the same $\Gamma_{L(R)}$, the ratio of $(\Delta E)^2$ is ∼1.50 for methylcytosine (E_{HOMO} = −5.97 eV) and cytosine (E_{HOMO} = −6.14 eV), according to our calculations. This is attributed to the electron-donating character of methyl substituents that tend to increase the HOMO level of dCMP closer to the Au Fermi level and, thus, provide the smaller ΔE and accompanied larger single-molecule conductance of methyl-dCMP than that obtained for dCMP.[28] This value of $(\Delta E)^2$ is close to the conductance ratio $G_{\text{methlcytosine}}/G_{\text{cytosine}}$ = 123/78 ∼ 1.58 (Supporting Information Table S1). These levels of agreement are considered to be reasonably high considering the uncertainty in $\Gamma_{L(R)}$, which in turn suggest the important role of the energy barrier ΔE on the single-molecule conductance.

The single-molecule detection experiments were extended to another type of chemically modified DNA base, 8-oxo-deoxyguanosine (oxo-dG). This molecule is known as a biologically

dx.doi.org/10.1021/ja203839e |J. Am. Chem. Soc. 2011, 133, 9124–9128

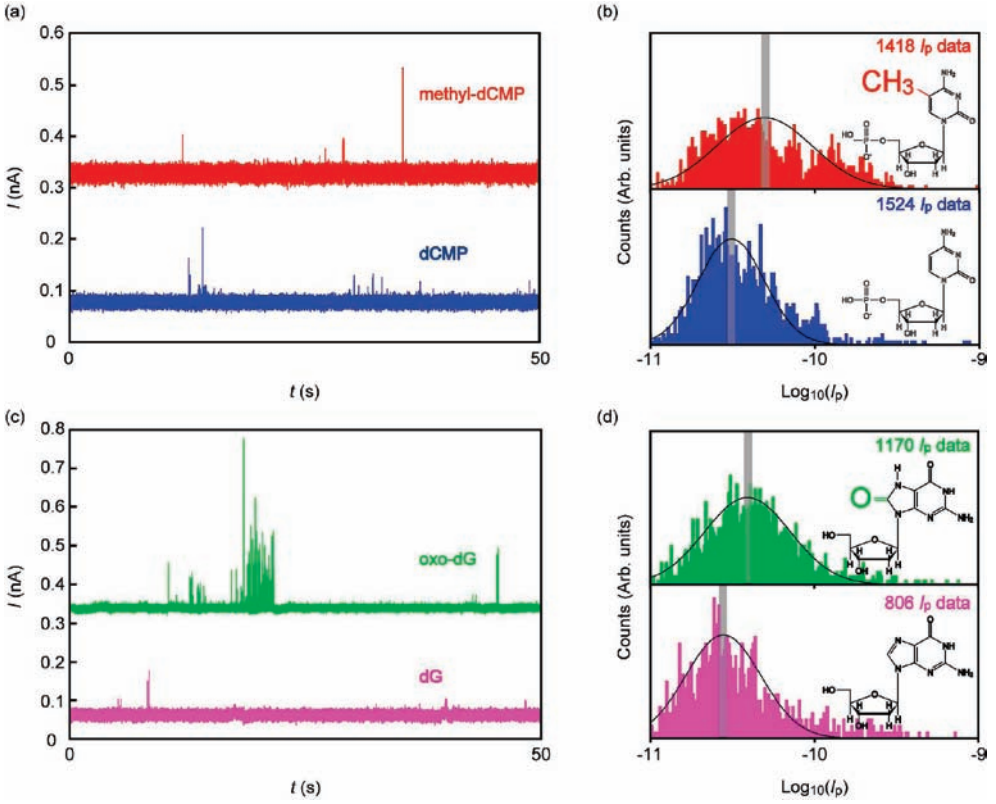

Figure 2. (a) Partial $I-t$ traces acquired in a solution of methyldeoxycytidine-5′-monophosphate (methyl-dCMP) (red), dCMP (blue), (c) 8-oxo-deoxyguanosine (oxo-dG) (green), and dG (purple) with 1 nm gap electrodes at 0.4 V. The curves are shifted vertically for clear visualization. (b) I_p distributions obtained from $I-t$ traces measured in an aqueous solution of methyl-dCMP (red), dCMP (blue), (d) oxo-dG (green), and dG (purple) at 0.4 V using 1 nm gap electrodes. Bin size is 0.01. Solid lines are the Gaussian fits.

important marker for assessing oxidative stress in humans relevant to aging and disease.[29] We observed current spikes suggestive of single-nucleotide trapping in an electrode gap (Figure 2c). The I_p histograms of these molecules reveal single-peak distributions (Figure 2d), from which we obtained single-molecule conductance of $G_{oxo\text{-}dG} = 98$ pS and $G_{dG} = 70$ pS for oxo-dG and dG, respectively, thus demonstrating single oxo-dG identifications by the tunneling conductance (Supporting Information Figure S2 and Figure 2d). The trend $G_{oxo\text{-}dG} > G_{dG}$ is in fact already expected from the DFT calculations on isolated molecules that predict a diminishment of ΔE of dG by about 0.1 eV from 0.46 to 0.38 eV through oxidation; quantitatively, this gives the $(\Delta E)^2$ ratio of about 1.46 for oxoguanine and guanine, which is in good agreement with $G_{oxoguanine}/G_{guanine} = 98/70 \sim 1.40$ (Supporting Information Table S1). These findings suggest a potential use of the transverse electron-transport technique for detections of virtually any type of DNA modification as any chemical substitutions would alter the molecular electronic structure at a certain extent.

Discrimination of Single Methylcytosines in a DNA Oligomer by Tunneling Current. It is of interest to evaluate the capability of the tunneling current technique for detecting single methylcytosines in a more realistic situation. Here, we exhibited the two-probe current measurements on a DNA oligomer having a sequence mCGmCG, where mC and G denote methyl-dCMP and dGMP, respectively (Figure 1a). This sequence was chosen as a model for a CpG island, the widely studied methylation sites in the vertebrate genome.[30] A reference molecule with a sequence of

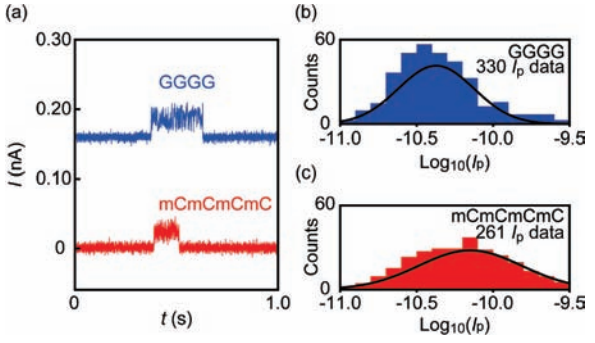

Figure 3. Electrical detection of a DNA oligomer with sequences of GGGG and mCmCmCmC. (a) Current signals obtained at 0.4 V in a Milli-Q solution of GGGG (blue) and mCmCmCmC (red) oligonucleotides. The base current is offset to zero. (b) I_p histograms of GGGG and (c) mCmCmCmC oligomers. Solid lines are Gaussian fitting to the current distributions.

GGGG was also employed. $I-t$ traces in a DNA 4-mer solutions (1 μM) show peculiar signals demonstrating anomalously long trapping duration (>0.1 s) (Figure 3a). The amount of net negative charge per molecule of 4-mer oligonucleotides is 4 times larger than that of the constituent monomers. From this it is inferred that the oligomer molecules feel a stronger electrostatic trapping force and tend to reside in the electrode gap for longer duration.[31,32] These traces thus render a tunneling current profile of the four-base sequence.

dx.doi.org/10.1021/ja203839e |J. Am. Chem. Soc. 2011, 133, 9124–9128

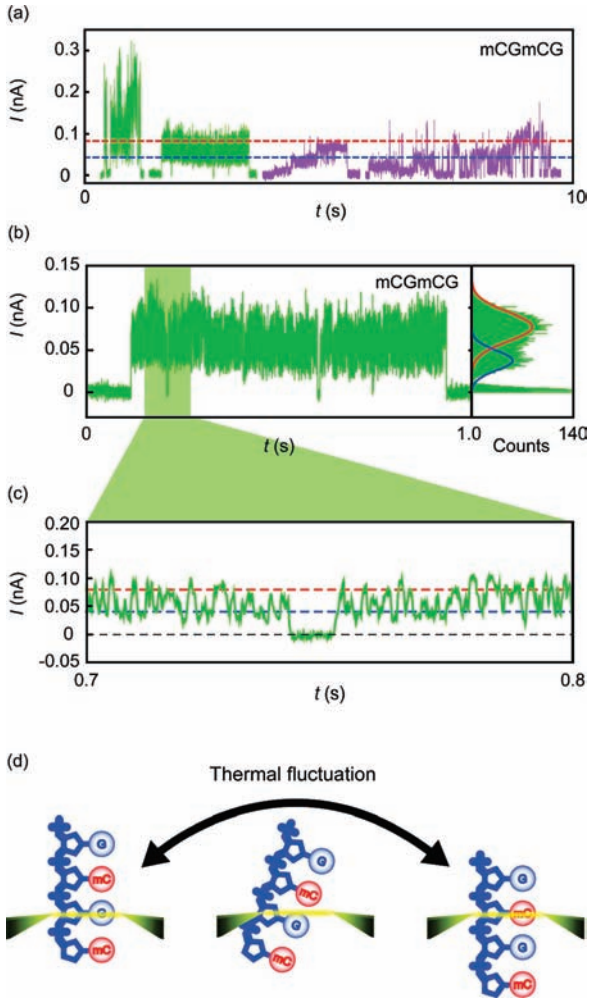

Figure 4. Tunneling current landscapes of a single-molecule DNA oligomer. (a) Current spikes showing long trapping durations of a single DNA oligomer with a sequence of mCGmCG at 0.4 V in a 1 nm electrode gap, where G and mC are dGMP and methyl-dCMP, respectively. The base current is offset to zero. Two types of signals were observed, one showing significant current fluctuations (green) and the other displaying multiple-step structures (purple). (b) A signal with current fluctuations. The right panel displays the corresponding current distributions of the $I-t$ traces binned at 1 pA. Solid lines are the Gaussian fits revealing two conductance states ascribable to G (blue) and mC (red). (c) A magnified view of panel b reveals two-level current fluctuations. (d) A possible mechanism that explains the characteristic current fluctuations in panel b. The left and right illustrations describe a measurement of current flowing through G and mC in the oligomer, respectively. Thermal fluctuations induce switching of an oligomer molecule between these two configurations in the electrode gap, whereby causing a large current fluctuation. The occasional drops of I to zero are probably due to a temporal decoupling of the electrode−molecule links (the model shown in the middle).

The single-molecule tunneling current landscapes allow electrical identifications of G and mC in the 4-mer oligonucleotide. Current spikes in GGGG and mCmCmCmC oligomers had single-step features (Figure 3a). The corresponding I_p histograms (Figure 3, parts b and c) reveal single-peak distributions centered at $I_{GGGG} \sim 42$ pA and $I_{mCmCmCmC} \sim 71$ pA for DNA oligomers with GGGG and mCmCmCmC sequences, respectively. In contrast, in addition to single-step current spikes,

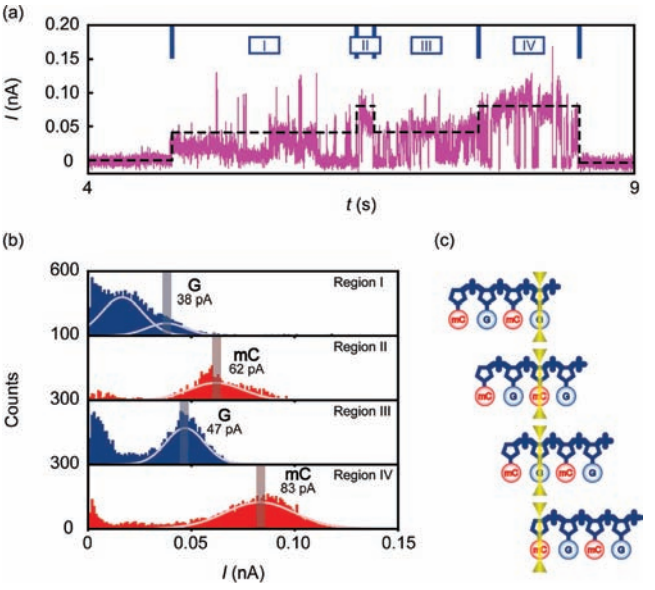

Figure 5. Partial sequencing of oligonucleotides. (a) An oligomer signal obtained for mCGmCG showing several plateaus at two current levels corresponding to the single-molecule conductance states of mC and G. The broken line is a guide to the eyes for the characteristic stepwise feature. (b) Partial histograms built with $I-t$ data in the four regions indicated in panel a. Bin size is 1 pA. Solid lines are Gaussian fits to the distributions. (c) A model for sequential reading of mCGmCG bases described to account for the particular current trace in panel a.

$I-t$ traces of mCGmCG oligonucleotides showed multiple-step signals (Figure 4a). Statistically, more than 70% of the current spikes obtained in a GmCGmC oligomer solution were of a single-step form. These signals can be ascribed to an oligomer passing by the electrode gap via Brownian motion with one of the constituent nucleobases being trapped/detrapped. The remaining 30% showed multistep structures suggesting multibase detection of a single oligonucleotide. Among the signals, about 70% exhibited current fluctuations (green curves in Figure 4, parts a and b). A closer look at this peculiar current profile reveals transitions between two particular current states (Figure 4c), which can be attributed to thermally activated switching of the molecular bridge between two distinct configurations. The corresponding I histogram shows two peaks located approximately at I_{GGGG} and $I_{mCmCmCmC}$ (right panel of the $I-t$ curve in Figure 4b). This elucidates the random nature of nucleobase positioning with respect to the electrodes (Figure 4d).[33]

Partial Sequencing of Oligonucleotides. Mapping a methylation pattern requires a sequential single-base profiling of a DNA so as to determine the exact positions of the methylated bases within the sequence. Occasionally, the signals reveal clear plateaus at two distinct levels corresponding to the electrical conductance of mC and G (purple traces in Figure 4a). Within these, about 90% showed two or three plateaus (for instance, the third curves from left in Figure 4a), indicative of partial sequencing of a GmCGmC oligomer. Although a very limited case, we also found signals composed of four plateaus (Figure 5a). Current histograms of the four segments give peak currents that are close to I_{GGGG} and $I_{mCmCmCmC}$ (Figure 5b). This four-plateau tunneling landscape implies full sequencing of the 4-mer oligonucleotides as modeled in Figure 5c, although we cannot rule out the possibility of the molecule going back and forth in the electrode gaps. The low probability of having long read reflects the

dx.doi.org/10.1021/ja203839e | J. Am. Chem. Soc. 2011, 133, 9124–9128

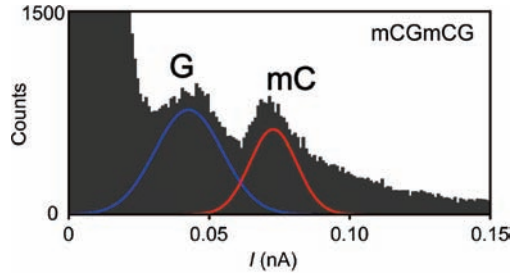

Figure 6. Statistical identification of methylcytosines in a single-molecule DNA oligomer: histogram constructed with consecutive I data of 47 signals. Bin size is 1 pA. Solid lines are Gaussian fits to the distribution (I_{low} and I_{high} were extracted from the peak positions of the blue and the red fitted distributions).

fact that the oligomer molecules move in and out of the electrode gap with a random conformation via the Brownian motion. Nonetheless, these results serve to suggest the utility of the tunneling current method for mapping the methylation pattern in a genome. Future effort should be directed toward regulation of the dynamic flow of a DNA through the electrode gap[34,35] so as to accomplish high-throughput mapping of methylation sites.

Statistical Identification of Single Methylcytosines in a DNA Oligomer. A current histogram constructed with 47 spike-like signals acquired for mCGmCG oligomers gives a double-peak current histogram (Figure 6). These peaks are located at $I_{low} \sim 43$ pA and $I_{high} \sim 73$ pA. From the fact that $I_{low(high)} \sim I_{GGGG(mCmCmCmC)}$, we can assign I_{low} and I_{high} to the single-molecule conductance states of G and mC, respectively, thereby demonstrating single-molecule discrimination of methylcytosine embedded in the 4-mer DNA.

CONCLUSION

In summary, we performed electrical detections of methyl-substituted nucleobases embedded in a short DNA using a nucleotide-sized electrode gap. We obtained tunneling current profiles of 4-mer methylated oligonucleotides. Statistical analysis of the tunneling current traces enabled identifications of methylated cytosines in the sequence. This illustrates the potential of the tunneling current approach for DNA methylation mapping.

ASSOCIATED CONTENT

Supporting Information. Electrode gap formation, single-dGMP conductance measurements, and complete refs 5 and 8. This material is available free of charge via the Internet at http://pubs.acs.org.

AUTHOR INFORMATION

Corresponding Author
taniguti@sanken.osaka-u.ac.jp

ACKNOWLEDGMENT

This research is partially supported by the Japan Society for the Promotion of Science (JSPS) through its funding program for World-Leading Innovative R&D on Science and Technology.

REFERENCES

(1) Strahl, B.; Allis, C. D. *Nature* **2000**, *403*, 41.
(2) Ruthenburg, A. J.; Li, H.; Patel, D. J.; Allis, C. D. *Nat. Rev. Mol. Cell Biol.* **2007**, *8*, 983.
(3) Alexander, R. P.; Fang, G.; Rozowsky, J.; Snyder, M.; Gerstein, M. B. *Nat. Rev. Genet.* **2010**, *11*, 559.
(4) Meissner, A.; Mikkelsen, T. S.; Gu, H.; Wernig, M.; Hanna, J.; Sivachenko, A.; Zhang, X.; Bernstein, B. E.; Nusbaum, C.; Jaffe, D. B.; Gnirke, A.; Jaenisch, R.; Lander, E. S. *Nature* **2008**, *454*, 766.
(5) Lister, R.; et al. *Nature* **2009**, *462*, 315.
(6) Baker, M. *Nat. Methods* **2010**, *7*, 181.
(7) Bock, C.; Tomazou, E. M.; Brinkman, A. B.; Müller, F.; Simmer, F.; Gu, H.; Jäger, N.; Gnirke, A.; Stunnenberg, H. G.; Meissner, A. *Nat. Biotechnol.* **2010**, *28*, 1106.
(8) Branton, D.; et al. *Nat. Biotechnol.* **2008**, *26*, 1146.
(9) Zwolak, M.; Di Ventra, M. *Rev. Mod. Phys.* **2008**, *80*, 141.
(10) Clarke, J.; Wu, H.-C.; Jayasinghe, L.; Patel, A.; Reid, S.; Bayley, H. *Nat. Nanotechnol.* **2009**, *4*, 265.
(11) Lindsay, S. M.; Thundat, T.; Nagahara, L. A.; Knipping, U.; Rill, R. L. *Science* **1989**, *244*, 1063.
(12) Xu, B.; Zhang, P.; Li, X.; Tao, N. *Nano Lett.* **2004**, *4*, 1105.
(13) van Zalinge, H.; Schiffrin, D. J.; Bates, A. D.; Haiss, W.; Ulstrup, J.; Nichols, R. J. *Chem. Phys. Chem.* **2006**, *7*, 94.
(14) Shapir, E.; Cohen, H.; Calzolari, A.; Cavazzoni, C.; Ryndyk, D. A.; Cuniberti, G.; Kotlyar, A.; Felice, R. D.; Porath, D. *Nat. Mater.* **2008**, *7*, 68.
(15) Tanaka, H.; Kawai, T. *Nat. Nanotechnol.* **2009**, *4*, 518.
(16) Chang, S.; Huang, S.; He, J.; Liang, F.; Zhang, P.; Li, S.; Chen, X.; Sankey, O.; Lindsay, S. *Nano Lett.* **2010**, *10*, 1070.
(17) Lindsay, S.; He, J.; Sankey, O.; Hapala, P.; Jelinek, P.; Zhang, P.; Chang, S.; Huang, S. *Nanotechnology* **2010**, *21*, 262001.
(18) Tsutsui, M.; Taniguchi, M.; Yokota, K.; Kawai, T. *Nat. Nanotechnol.* **2010**, *5*, 286.
(19) van Ruitenbeek, J. M.; Alvarez, A.; Pineyro, I.; Grahmann, C.; Joyez, P.; Devoret, M. H.; Esteve, D.; Urbina, C. *Rev. Sci. Instrum.* **1996**, *67*, 108.
(20) Agraït, N.; Yeyati, A. L.; van Ruitenbeek, J. M. *Phys. Rep.* **2003**, *377*, 81.
(21) Tsutsui, M.; Shoji, K.; Taniguchi, M.; Kawai, T. *Nano Lett.* **2008**, *8*, 345.
(22) Tsutsui, M.; Taniguchi, M.; Kawai, T. *Appl. Phys. Lett.* **2008**, *93*, 163115.
(23) Venkataraman, L.; Klare, J. E.; Nuckolls, C.; Hybertsen, M. S.; Steigerwald, M. L. *Nature* **2006**, *442*, 904.
(24) Xiao, X.; Xu, B.; Tao, N. J. *Nano Lett.* **2004**, *4*, 267.
(25) Lagerqvist, J.; Zwolak, M.; Di Ventra, M. D. *Biophys. J.* **2007**, *93*, 2384.
(26) Lindsay, S. M.; Ratner, M. A. *Adv. Mater.* **2007**, *19*, 23.
(27) Chen, F.; Tao, N. J. *Acc. Chem. Res.* **2009**, *42*, 429.
(28) Venkataraman, L.; Park, Y. S.; Whalley, A. C.; Nuckolls, C.; Hybertsen, M. S.; Steigerwald, M. L. *Nano Lett.* **2007**, *7*, 502.
(29) David, S. S.; O'Shea, V. L.; Kundu, S. *Nature* **2007**, *447*, 941.
(30) Laird, P. W. *Nat. Rev. Genet.* **2010**, *11*, 191–203.
(31) Bezryadin, A.; Dekker, C.; Schmid, G. *Appl. Phys. Lett.* **1997**, *71*, 1273.
(32) Ai, Y.; Liu, J.; Zhang, B.; Qian, S. *Anal. Chem.* **2010**, *82*, 8217.
(33) Huang, S.; He, J.; Chang, S.; Zhang, P.; Liang, F.; Li, S.; Tuchband, M.; Fuhrmann, A.; Ros, R.; Lindsay, S. *Nat. Nanotechnol.* **2010**, *5*, 868.
(34) Keyser, U. F.; Koeleman, B. N.; van Dorp, S.; Krapf, D.; Smeets, R. M. M.; Lemay, S. G.; Dekker, N. H.; Dekker, C. *Nat. Phys.* **2006**, *2*, 473.
(35) Wanunu, M.; Morrison, W.; Rabin, Y.; Grosberg, A. Y.; Meller, A. *Nat. Nanotechnol.* **2010**, *5*, 160.